Ultra-Widefield Imaging of the Retinal Macrovasculature in Parkinson Disease Versus Controls With Normal Cognition Using Alpha-Shapes Analysis

Ma, Justin P.; Robbins, Cason B.; Pead, Emma; McGrory, Sarah; Hamid, Charlene; Grewal, Dilraj S.

Published in:
Translational Vision Science and Technology

DOI:
10.1167/tvst.13.1.15

Publication date:
2024

tvst

Refractive Intervention

Ultra-Widefield Imaging of the Retinal Macrovasculature in Parkinson Disease Versus Controls With Normal Cognition Using Alpha-Shapes Analysis

Justin P. Ma[1,2], Cason B. Robbins[1,2], Emma Pead[3], Sarah McGrory[3], Charlene Hamid[3], Dilraj S. Grewal[1,2], Burton L. Scott[1,4], Emanuele Trucco[5], Tom J. MacGillivray[3,*], and Sharon Fekrat[1,2,4,*]

[1] iMIND Study Group, Duke University School of Medicine, Durham, NC, USA
[2] Department of Ophthalmology, Duke University School of Medicine, Durham, NC, USA
[3] VAMPIRE Project, Centre for Clinical Brain Science, University of Edinburgh, Edinburgh, UK
[4] Department of Neurology, Duke University School of Medicine, Durham, NC, USA
[5] VAMPIRE Project, University of Dundee, Dundee, UK

Correspondence: Sharon Fekrat, Department of Ophthalmology, Duke University School of Medicine, 2531 Erwin Rd., DUMC Box 3802, Durham, NC 27705, USA. e-mail: sharon.fekrat@duke.edu

Received: April 18, 2023
Accepted: December 13, 2023
Published: January 17, 2024

Keywords: imaging; neurodegeneration; Parkinson disease; retina

Citation: Ma JP, Robbins CB, Pead E, McGrory S, Hamid C, Grewal DS, Scott BL, Trucco E, MacGillivray TJ, Fekrat S. Ultra-widefield imaging of the retinal macrovasculature in parkinson disease versus controls with normal cognition using alpha-shapes analysis. Transl Vis Sci Technol. 2024;13(1):15, https://doi.org/10.1167/tvst.13.1.15

Purpose: To investigate retinal vascular characteristics using ultra-widefield (UWF) scanning laser ophthalmoscopy in Parkinson disease (PD).

Methods: Individuals with an expert-confirmed clinical diagnosis of PD and controls with normal cognition without PD underwent Optos California UWF imaging. Patients with diabetes, uncontrolled hypertension, glaucoma, dementia, other movement disorders, or known retinal or optic nerve pathology were excluded. Images were analyzed using Vasculature Assessment and Measurement Platform for Images of the Retina (VAMPIRE-UWF) software, which describes retinal vessel width gradient and tortuosity, provides vascular network fractal dimensions, and conducts alpha-shape analysis to further characterize vascular morphology (complexity, Opα_{min}; spread, OpA).

Results: In the PD cohort, 53 eyes of 38 subjects were assessed; in the control cohort, 51 eyes of 33 subjects were assessed. Eyes with PD had more tortuous retinal arteries in the superotemporal quadrant ($P = 0.043$). In eyes with PD, alpha-shape analysis revealed decreased OpA, indicating less retinal vasculature spread compared to controls ($P = 0.032$). Opα_{min} was decreased in PD ($P = 0.044$), suggesting increased vascular network complexity. No differences were observed in fractal dimension in any region of interest.

Conclusions: This pilot study suggests that retinal vasculature assessment on UWF images using alpha-shape analysis reveals differences in retinal vascular network spread and complexity in PD and may be a more sensitive metric compared to fractal dimension.

Translational Relevance: Retinal vasculature assessment using these novel methods may be useful in understanding ocular manifestations of PD and the development of retinal biomarkers.

Introduction

Parkinson disease (PD) is a neurodegenerative condition characterized by dysfunction of the substantia nigra due to loss of dopaminergic neurons.[1] As the second most common neurodegenerative disease after Alzheimer disease, PD often manifests clinically with motor signs and symptoms including rigidity, bradykinesia, and resting tremor.[2] The non-motor features of PD include depression, anxiety, constipation, and disrupted sleep, in addition to sensory complaints such as visual dysfunction and ultimately cognitive decline.[1,3–6] As an extension of the brain, the eye has become an organ of interest in the study of neurodegeneration. Tissue-level evidence of alpha-synuclein

deposition, a key pathologic marker of PD, has been demonstrated in the retina along with ganglion cell dysfunction and thinning of the retinal nerve fiber layer, suggesting that further investigation into associated ophthalmic findings is warranted to improve our understanding of both the disease and its diagnosis.[7–10]

Although the primary pathophysiology of neurodegenerative disease is thought to be distinct from cerebrovascular diseases, there is growing consensus on the impact of the "neurovascular" components of neurodegenerative disease.[11,12] Microvascular effects and reduced cerebral blood flow have been characterized in a variety of neurodegenerative conditions.[11] In individuals with PD, endothelial cell abnormalities and capillary injury—as indicated by shorter vessel lengths, fewer capillary vessels, larger vessel diameters, and decreased vessel branching—have been described in multiple regions of the brain.[13]

Vascular pathology in the brain has been associated with PD, but how these factors manifest in the vasculature of the closely related neurosensory retinal tissue is an emerging field of inquiry.[14,15] As the retina is one of the rare locations of the body where blood vessels are directly visible to the examiner, imaging modalities such as optical coherence tomography angiography (OCTA), fundus photography, and scanning laser ophthalmoscopy (SLO) offer the unique opportunity to assess and quantify retinal vascular pathology with non-invasive, high-resolution imaging.[16–18] Studies using OCT and OCTA have shown a smaller foveal avascular zone (FAZ) and decreased retinal perfusion density in PD compared to controls, although more work is needed to further define these relationships.[17,19–22] Studies using even standard fundus photography and convolutional neural networks without a focus on vascular parameters are still fledgling, and, in general, exploration of newly applied imaging modalities and clinical correlation may become instrumental in improving our understanding of the role of ocular diagnostics in neurodegenerative disease.[23,24]

Previous studies using other retinal imaging modalities such as fluorescein angiography, OCT, and OCTA have reported differences in the retinal microvasculature in eyes of individuals with PD.[25–27] Although FAZ area has been shown to increase with age in some studies, a significantly smaller FAZ area has been measured in patients with PD compared to controls using fluorescein angiography and OCTA.[21,28–30] Kwapong and colleagues[20] reported a significantly lower retinal microvascular density using macular OCTA in 38 patients with PD. Other studies have noted abnormalities in the retinal microvasculature in PD using OCTA, including decreased capillary skeleton and perfusion and vessel densities, as well as changes in choroidal structure.[19,31] The aforementioned studies reported changes at the microvascular capillary level, whereas we assessed the larger retinal vessels at the level of the arteries and veins. Furthermore, macular-centered studies using OCT and OCTA modalities focusing upon the FAZ and other microvascular parameters do not generally assess qualities of the retinal periphery, and our UWF analysis aims to bolster our understanding of this disease with new perspective. Unique patterns of retinal vasculature complexity differences on UWF images have not been previously reported.

Although UWF SLO images are essentially en face images without the volumetric dimension of OCT modalities, they are able to characterize the retinal vascular network to a wider extent. Moreover, although OCT/OCTA may capture the microvascular networks in the capillary plexuses, the goal of this study was to investigate the larger vessels of the arterioles and venules of the macrovascular network. Compared to conventional SLO or fundus cameras that capture only 30° to 45°, UWF SLO captures images of the retina with an angular view of up to 200°. This is far wider than that of OCT modalities at 20-30° and some OCTA modalities at 10°, and even wider than that of widefield OCT technologies at 100°.[32] Furthermore, the shorter acquisition times of UWF SLO may be more facile and accessible for patients, and the larger field of view of the retinal vasculature may present the chance for more comprehensive and efficient study of the microvasculature in the PD population. As such, UWF SLO was selected as the imaging modality for this study, and further investigation may demonstrate this method as a potentially useful adjunct in multimodal approaches to the ocular study of neurodegenerative disease.

The application of UWF fundus imaging to study the vasculature in PD remains a novel area of inquiry. Ophthalmic biomarkers have potential as an adjunct to the currently utilized Movement Disorders Society Clinical Diagnostic Criteria for the diagnosis of PD.[33,34] We examined the retinas of patients with PD using UWF imaging and compared them to those of controls with normal cognition without PD to investigate retinal vascular differences that might contribute to the development of novel imaging-derived biomarkers.

Methods

This cross-sectional study (ClinicalTrials.gov identifier NCT03233646) was approved by the Duke Health

Institutional Review Board (Pro00082598), adhered to the tenets of the Declaration of Helsinki with regard to human subjects, and complied with the Health Insurance Portability and Accountability Act of 1996.

Study Participants

Individuals were enrolled from the Duke Movement Disorders Clinics. Patients with a clinical diagnosis of PD who met Disorders Society Clinical Diagnostic Criteria, confirmed by an experienced neurologist (BLS) with expertise in the diagnosis and treatment of PD, were identified. These patients were compared to a control cohort of volunteers who did not have a history of tremor or cognitive dysfunction, or motor symptoms consistent with Parkinsonism. To avoid confounding any observed relationship between retinal changes and PD, exclusion criteria included uncontrolled hypertension, diabetes mellitus, glaucoma, retinal or optic nerve disease, non-PD dementia, demyelinating disorders, or corrected visual acuity worse than 20/40 on the day of image acquisition. All subjects underwent cognitive screening with a Mini-Mental State Examination (MMSE) on the day of study enrollment, and all subjects in both the control and PD groups scored 26 or above, within the original normal screening range (25 or greater). Participants were recruited between August 2017 and June 2022. Participants and images were de-identified after initial imaging for general use during data curation, quality control, and analysis; however, it would still have been possible to identify a given image if necessary.

Image Acquisition and Retinal Vessel Parameters

The UWF images were acquired with Optos California SLO (Optos, Marlborough, MA) and manually screened by trained study staff (JPM, SM, CH, EP) for image quality to exclude those images that had artifacts or reflections, media opacity, eyelid or eyelash artifacts that crossed the bounds of each region of interest (ROI), or were out of focus, as these issues would interfere with image analysis. Image postprocessing included stereographic projection of the curved surface of the retina allowing for linear measurement of distance (e.g., vessel width). Images with abnormal projection resulting from poor patient fixation or errors in automated anatomic recognition by the processing software were excluded, as these would lead to erroneous measurements.[35] Measurements of the retinal vasculature were obtained using bespoke software (Vasculature Assessment Platform for Images of the Retina; version VAMPIRE-UWF, Universities of Edinburgh and Dundee, UK) specifically designed for analysis of UWF images.[36,37]

First, a manually drawn elliptical ROI was annotated by experienced masked reviewers (CH, SM) to exclude eyelashes and eyelids that obscured peripheral parts of the image. Next, the vessels were automatically segmented within the manually drawn ROI and divided into superotemporal, inferotemporal, inferonasal, and superonasal quadrants (defined as two perpendicular lines: one through the optic disc center and the other through the optic disc center and fovea within the manual ROI).[37] The reviewers manually selected the largest and longest artery and vein pair within each quadrant; vessel widths and tortuosity were extracted from these annotated vessel paths.[37,38] To characterize how vessel width changes as it continues from the optic disk toward the retinal periphery, the gradient of the robust regression line that fit the measurements of vessel width (in microns) against the distance along the path (in millimeters), denoted as width gradient, was computed.

We quantified vascular network morphology within a standardized ROI for UWF images that sampled the same area within each UWF image. The standardized ROI has been defined as the intersection of manually drawn ROIs within the dataset utilizing a protocol described in the cited study by Pead and colleagues,[39] representing an approximately ellipsoid area of 25 mm by 18 mm in dimension or 120° by 85° of angular view. The standardized ROI was utilized to define a consistent anatomical area for measurement internal to both fractal dimensions and alpha shapes and to avoid any confounding effect of ROI placement and space between the two parameters. Moreover this was defined to reduce the effect of ROI placement on fractal dimension measures specifically while maximizing the area that was unobstructed and therefore could be measured within a UWF image.[40,41] The standardized ROI was subdivided into posterior ROI (an annulus centered on the optic disc, extending 2 disk diameters from the edge of the disc) and midperiphery ROI (a ring located peripheral to the posterior ROI but within the peripheral boundary of the standardized ROI) (Fig. 1).[42] After computerized detection of vessels (Vampire-UWF),[37] fractal dimension as a measurement of retinal vessel branching complexity was computed in the standardized ROI, posterior ROI, and midperiphery ROI.[43] Further measures of retinal vessel morphology were conducted within the standardized ROI using alpha shapes (Fig. 2), a method that extracts an additional measure of vessel complexity ($Op\alpha_{min}$) and vessel spread (OpA).[41]

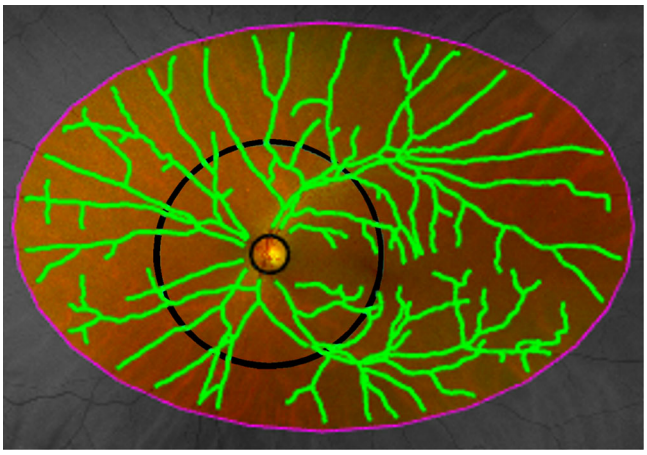

Figure 1. Schematic of the VAMPIRE zones. The standardized ROI (pink oval) is further subdivided into the posterior ROI (bounded by the black circles, excluding the optic disk) and the midperiphery ROI (between the outer black circle and pink oval). Segmentation and skeletonization of the retinal vasculature (1-pixel-wide green curved lines) were automated.

Statistical Analysis

Data analysis was completed using SAS 9.4 (SAS Institute, Cary, NC). Multivariable generalized estimating equation (GEE) models that accounted for within-subject correlation (i.e., two eyes of an individual) were used to compare retinal vessel parameters and a known diagnosis of PD. GEE models were adjusted for age and sex as covariates testing the null hypothesis of parameter difference between groups as equal to zero with an alpha significance level < 0.05.

Results

Initial imaging included 104 eyes of 71 PD subjects and 82 eyes of 55 control subjects. Exclusion of poor-quality images yielded a PD group of 53 eyes of 38 participants and a control group consisting of 51 eyes of 33 participants. Demographic characteristics are presented in Table 1. The mean age of those in the PD

Table 1. Demographics

Statistic	Parkinson	Controls	*P*
Subjects (eyes), n	38 (53)	33 (51)	—
Age (y)			
Mean (SD)	66.7 (7.5)	70.8 (5.7)	0.012[a]
Minimum, median, maximum	51, 66.1, 85.4	57.8, 71.0, 82.7	
Male, n (%)	23 (61)	18 (56)	0.638[b]

[a]Based on *t*-test of difference between means.
[b]Based on χ^2 test of difference between proportions.

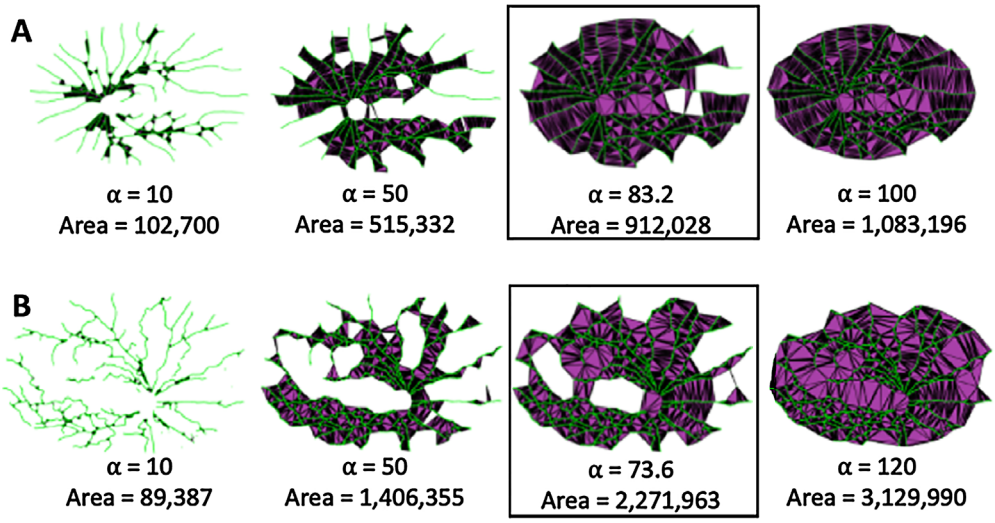

Figure 2. Measurement of alpha shapes within the standardized ROI retinal vasculature on UWF images. As α increases, more edges of the Delaunay triangularization (DT) are included until eventually all edges of the DT are included (*far right*). This image includes image set A, which is a PD example, and image set B, which is an example of a cognitively normal control without PD. The α-shape for each individual (*black box*) is constructed from the minimum value of α that encompasses all points, giving a topological outline of the retinal vascular skeleton. Individual A has a higher Opα_{min} and OpA ($\alpha = 83.2$ pixels and area = 912,028 pixels, respectively) compared to individual B ($\alpha =$ 73.6 pixels and area = 2,271,963 pixels, respectively), suggesting a relatively complex and dispersed vasculature in B compared to A. Opα_{min} (α) refers to the minimum such radius (Opα) that is required to encircle the nodes of a network in an alpha-shapes analysis, a measure of network complexity. OpA (area) refers to the total area spanned by the vascular network, a measure of spread.

Table 2. Retinal Vessel Width Gradient

Statistic	Parkinson ($n = 53$ Eyes)	Controls ($n = 51$ Eyes)	P[a]
Superotemporal arteriolar			
Mean (SD)	−0.00336 (0.00119)	−0.00339 (0.00089)	0.956
Minimum, median, maximum	−0.00780, −0.00309, −0.00134	−0.00520, −0.00323, −0.00157	
Superotemporal venular			
Mean (SD)	−0.00416 (0.00092)	−0.00425 (0.00099)	0.712
Minimum, median, maximum	−0.00658, −0.00408, −0.00196	−0.00655, −0.00419, −0.00256	
Inferotemporal arteriolar			
Mean (SD)	−0.00283 (0.00093)	−0.00298 (0.00079)	0.902
Minimum, median, maximum	−0.00554, −0.00280, −0.00023	−0.00467, −0.00292, −0.00107	
Inferotemporal venular			
Mean (SD)	−0.00404 (0.00125)	−0.00381 (0.00109)	0.878
Minimum, median, maximum	−0.00696, −0.00387, −0.00152	−0.00679, −0.00369, −0.00099	
Inferonasal arteriolar			
Mean (SD)	−0.00316 (0.00153)	−0.00356 (0.00158)	0.531
Minimum, median, maximum	−0.00703, −0.00310, −0.00010	−0.00929, −0.00334, −0.00095	
Inferonasal venular			
Mean (SD)	−0.00406 (0.00137)	−0.00410 (0.00146)	0.803
Minimum, median, maximum	−0.00769, −0.00395, −0.00155	−0.00770, −0.00396, −0.00126	
Superonasal arteriolar			
Mean (SD)	−0.00257 (0.00103)	−0.00244 (0.00115)	0.105
Minimum, median, maximum	−0.00659, −0.00242, −0.00060	−0.00500, −0.00224, −0.00023	
Superonasal venular			
Mean (SD)	−0.00329 (0.00142)	−0.00304 (0.00114)	0.102
Minimum, median, maximum	−0.00707, −0.00315, −0.00022	−0.00593, −0.00305, −0.00082	

[a]P values are based on GEEs for testing differences between group means equal to zero, adjusted for age and sex.

group was 66.7 years, with a standard deviation (SD) of 7.5 years. Those in the control group had a mean age ± SD of 70.8 ± 5.7 years and were significantly older than the PD group ($P = 0.012$). The PD group was 61% male (23/38 subjects), and the control group was 56% male (18/33 subjects) ($P = 0.638$). There was no evidence of significant differences in retinal vessel width gradient between the PD cohort and the control group (Table 2). Vessels were stratified as arterial and venous as well as by image quadrant (Table 2).

There was a trend of more tortuous retinal arteries in the superotemporal quadrant with an age- and sex-adjusted P value for the PD cohort versus control cohort of 0.043 (Table 3). There were no differences in arterial or venous tortuosity in any other quadrant. There was no significant difference in fractal dimension in any ROI in PD compared to controls. Age- and sex-adjusted P values comparing fractal dimension were 0.293 within the standardized ROI, 0.946 within the posterior ROI, and 0.270 within the midperiphery ROI (Table 4).

Applying alpha-shape analysis, the PD cohort exhibited smaller OpA (smaller area, $P = 0.032$) and smaller $\mathrm{Op}\alpha_{\min}$ (vascular network complexity, $P = 0.044$) compared to the control cohort, after age- and sex-adjusted analysis (Table 5). Overall, this indicates a more complex vasculature that also covers a smaller area in the PD cohort.

Discussion

To our knowledge, this is the largest cohort of individuals with PD who have undergone retinal vessel analysis using UWF SLO with comparison to a cognitively normal cohort without PD. Those with PD had greater arterial tortuosity in the superotemporal quadrant. Alpha-shapes analysis indicated decreased spread of the overall retinal vasculature as measured by OpA and increased vascular network complexity as measured by $\mathrm{Op}\alpha_{\min}$.

We found no evidence of significant differences in the measurements of vessel width gradients; this is in loose concordance with prior related studies that measured vessel caliber using OCT. Although not

Table 3. Retinal Vessel Tortuosity

Statistic	Parkinson ($n = 53$ Eyes)	Controls ($n = 51$ Eyes)	P[a]
Superotemporal arteriolar			
Mean (SD)	0.0004449 (0.0015631)	0.0000357 (0.0000359)	0.043
Minimum, median, maximum	0.0000085, 0.0000343, 0.0099491	0.0000040, 0.0000263, 0.0001939	
Superotemporal venular			
Mean (SD)	0.0001075 (0.0003835)	0.0005111 (0.0027239)	0.275
Minimum, median, maximum	0.0000057, 0.0000315, 0.0027557	0.0000032, 0.0000303, 0.0192332	
Inferotemporal arteriolar			
Mean (SD)	0.0003854 (0.0016486)	0.0000980 (0.0003205)	0.244
Minimum, median, maximum	0.0000024, 0.0000329, 0.0117470	0.0000043, 0.0000306, 0.0022335	
Inferotemporal venular			
Mean (SD)	0.0001007 (0.0002845)	0.0002242 (0.0011049)	0.453
Minimum, median, maximum	0.0000093, 0.0000305, 0.0017512	0.0000035, 0.0000267, 0.0077612	
Inferonasal arteriolar			
Mean (SD)	0.0001378 (0.0007750)	0.0000182 (0.0000238)	0.241
Minimum, median, maximum	0.0000013, 0.0000158, 0.0056648	0.0000002, 0.0000088, 0.0001041	
Inferonasal venular			
Mean (SD)	0.0000250 (0.0000351)	0.0000156 (0.0000133)	0.138
Minimum, median, maximum	0.0000004, 0.0000158, 0.0001971	0.0000004, 0.0000123, 0.0000576	
Superonasal arteriolar			
Mean (SD)	0.0001487 (0.0005206)	0.0000189 (0.0000241)	0.069
Minimum, median, maximum	0.0000000, 0.0000204, 0.0026623	0.0000004, 0.0000114, 0.0001227	
Superonasal venular			
Mean (SD)	0.0000408 (0.0001014)	0.0000193 (0.0000155)	0.116
Minimum, median, maximum	0.0000006, 0.0000169, 0.0007057	0.0000005, 0.0000157, 0.0000869	

[a] P values are based on GEEs for testing differences between group means equal to zero, adjusted for age and sex.

Table 4. Fractal Dimension in Eyes of Individuals with Parkinson Disease Versus Controls

Statistic	Parkinson ($n = 53$ Eyes)	Controls ($n = 51$ Eyes)	P[a]
Standardized ROI			
Mean (SD)	1.402 (0.033)	1.406 (0.030)	0.293
Minimum, median, maximum	1.309, 1.408, 1.451	1.332, 1.411, 1.455	
Posterior ROI			
Mean (SD)	1.344 (0.036)	1.342 (0.045)	0.946
Minimum, median, maximum	1.244, 1.349, 1.412	1.227, 1.348, 1.419	
Midperiphery ROI			
Mean (SD)	1.330 (0.034)	1.335 (0.041)	0.270
Minimum, median, maximum	1.200, 1.336, 1.386	1.218, 1.341, 1.391	

[a] P values are based on GEEs for testing differences between group means equal to zero, adjusted for age and sex.

directly comparable to UWF imaging, assessing the retinal vasculature by quadrant on OCT and differentiating between arterial and venous supply have not shown evidence of change, although vessel diameter was uniformly decreased in patients with PD versus age- and sex-matched controls.[44] Kromer and colleagues[17] did not observe significant differences in retinal vessel diameter but did not comment on rate of change.

We observed greater arterial tortuosity in the superotemporal quadrant of eyes with PD compared to eyes of cognitively normal controls without PD. There was

Table 5. Alpha Shapes

Statistic	Parkinson ($n = 53$ Eyes)	Controls ($n = 51$ Eyes)	P[a]
Opα_{min}			
Mean (SD)	67.6 (12.6)	74.7 (17.9)	0.044
Minimum, median, maximum	49.2, 66.5, 102.8	45.5, 69.8, 120.0	
OpA			
Mean (SD)	695633 (167153)	767595 (170682)	0.032
Minimum, median, maximum	274,272, 702,898, 1,034,803	393,018, 783,543, 1,074,474	

Opα_{min} refers to the minimum radius (Opα) that is required to encircle the nodes of a network in an alpha-shapes analysis, a measure of network complexity. OpA refers to the total area spanned by the vascular network, a measure of spread.

[a]P values are based on GEEs for testing differences between group means equal to zero, adjusted for age and sex.

a trend toward greater tortuosity in the superonasal arteries, as well, in PD subjects, which may suggest that the superior retina might be an area of interest for future studies of individuals with PD. In general, vascular tortuosity has been associated with various ischemic phenomena in numerous organ systems.[45–47] In particular, arterial system tortuosity is often discussed in the context of cerebrovascular disease and aging.[48,49] Measuring vascular tortuosity as a potential marker of cellular stress in the retina and understanding the mechanism and pathophysiology of retinal vascular tortuosity in association with PD and other neurodegenerations are nascent areas of investigation, and it remains unclear whether vascular tortuosity in the retina is a primary or secondary phenomenon in the context of PD.[45,50] Some studies in Alzheimer disease have also reported increased vessel tortuosity in the venous tree, although without distinction by quadrant; however, there are no similar studies yet in PD.[51,52] The observed increased tortuosity solely in the retinal arterial system may be related to a parallel mechanism of retinal vascular stress in PD, either through suggested effects of alpha-synuclein clearance via periarterial pathways which may be perturbed in PD or perhaps via some less specific anomaly in the constitutive expression of alpha-synuclein in the central nervous system vascular walls.[53,54]

We found a smaller OpA in PD, which indicates decreased spread of retinal vessels in this cohort, and a smaller Opα_{min} (a smaller radius required to refine the skeleton of the vessel segmentation during triangularization), which geometrically suggests a retinal vascular network morphology of increased complexity in eyes with PD. As the architecture of the microvasculature represents a physiologic optimization of energy cost and perfusion, perturbation of the normal morphology may be a marker of vascular stress secondary to neurodegeneration.[16,55] Our prior study of PD subjects using macular OCTA found decreased vessel density in the 6-mm × 6-mm Early Treatment Diabetic Retinopathy Study circle, which could represent some microvascular change in the highly metabolic and sensitive tissue of the macula by a similar mechanism.[31] Although the metrics and area measured with OCTA are not directly comparable to UWF fundus images, these data suggest that the vascular morphology changes in PD may extend beyond the central macula.

A prior study has shown lower retinal capillary complexity as described by fractal dimension, whereas our similar measure of complexity as measured by alpha-shapes analysis, Opα_{min}, specifically suggested increased complexity.[19] We speculate that perhaps early exhaustion of the capillary beds due to PD pathophysiology may cause early microvascular change, followed by macrovascular retraction, as suggested by decreased OpA, or spread, in the PD group. The chronology and pathophysiology of such a mechanism remain unclear. Even in more broadly studied diseases of both micro- and macrovascular components, such as diabetes, the true sequence and interplay between microvascular and macrovascular manifestations is not well defined.[56] Further study of differential changes between the vascular hierarchies may help elucidate the nuance of our findings in comparison to microvascular findings described by other work.

In comparison to the measurement of fractal dimension, alpha shapes are not space dependent in terms of ROI size. In our analysis, we standardized the fractal dimension zones to minimize the effect of ROI placement and size. Nonetheless, we did not find evidence of any differences in fractal dimension measures between groups, in contrast to alpha shapes, which did demonstrate significant changes. This suggests that alpha shapes could potentially capture structural nuances on UWF that are not described by fractal dimension

alone and could be a more useful metric in a multimodal assessment of retinal changes in PD. Fractal dimension measures the "space-filling" properties of a network, and alpha shapes measure the "shape" properties. They quantify inherently different characteristics of a network but are potentially complementary by nature, which alone could explain this difference. The degree of discrepancy and moreover the clinical significance of this observation will require further study. Future studies of larger datasets would aid in validating this novel parameter for broader use alongside other imaging modalities in a multimodal approach.

Data on other demographic factors that may have impacted parameters of the retinal vasculature, including socioeconomic status and ethnicity, were not available but may have had untold impact on the observations in this study. Furthermore, in our recruitment, few participants with advanced disease, based on PD disease staging with the Hoehn and Yahr scale, demonstrated severe disease, largely due to their inability to remain tremor-free for image acquisition. Only two eyes of two participants scored a 3 or greater severity on the Hoehn and Yahr scale, where a class 3 grade indicates mild to moderate disease with some postural instability while remaining physically independent. There remains an opportunity to conduct a deeper analysis of disease severity and retinal findings when participants can be recruited and reliable images obtained. In general, many studies of neurodegeneration, including our own, are limited to some degree by difficulty in controlling for the numerous lifestyle and health factors which are inherent to the lives of patients with these diagnoses, such as medication use, physical activity, and other comorbidities. Future larger and more advanced studies beyond our exploratory work may be able to more rigorously regulate the controls of comparison.

Although images of poor quality were excluded from our sample to allow for accurate analyses, the strict exclusion criteria may currently limit the generalizability of our observations to all individuals with PD which would otherwise be inclusive of persons who cannot provide high-quality images, although a sufficient number of good quality images would be necessary for the development of a clinically relevant retinal biomarker. Although the Optos device software accounted for the curvature of the retina by projecting to a standard eye model, it does not account for irregularly shaped eyes and deviations in posterior curvature from the standard model, which could introduce error. Patients with high refractive error (+6 or –6 diopters) were excluded from this study to minimize distortion-related effects on image analysis. Although the literature generalizes such effects to high refractive error, it is possible that variation in axial length even within this range may have had some, albeit minimal, effect on image measurements.[57] The inclusion of axial length measurements may bolster future analyses. In addition, although the angular view of the standardized ROI, at 120° by 85°, exceeds that of other conventional imaging such as non-UWF fundus photography and OCT, the unused image area represents an opportunity to further improve this analytical platform. With regard to the potentially disproportionate number of images included in the study that met inclusion criteria in the PD group (51%) versus the control group (65%), a χ^2 statistic assuming independence of group status and eye exclusion yields a non-significant $P = 0.1255$. However, to explain the higher proportion of excluded images, we postulate a tendency for patients with PD to have more eyelid and eyelash artifacts due to poor facial muscle control and subtle motion artifacts related to PD motor symptoms.

In this study, our findings suggest that there are significant differences in the retinal vasculature morphology captured on UWF fundus images using the novel application of alpha-shape analysis in patients with PD compared to controls with normal cognition. These differences included increased superotemporal quadrant arterial tortuosity in subjects with PD, decreased vascular spread (OpA), and increased vascular network complexity (lower $\mathrm{Op}\alpha_{\mathrm{min}}$). Continued investigation into the utility of UWF imaging is warranted to further explore and define novel biomarkers for PD and the potential adjunctive role of alpha-shapes analysis in a multimodal approach to ophthalmic imaging in neurodegenerative disease. Future studies in automation may eliminate the need for manual image annotation and for vessel arteriolar–venular differentiation.

Acknowledgments

Our additional acknowledgments go to the members of the iMIND Study Group Team who were involved in some capacity in this work. Study team members may be found at https://dukeeyecenter.duke.edu/imind-team.

Disclosure: **J.P. Ma**, None; **C.B. Robbins**, None; **E. Pead**, None; **S. McGrory**, None; **C. Hamid**, None; **D.S. Grewal**, None; **B.L. Scott**, None; **E. Trucco**, None; **T.J. MacGillivray**, None; **S. Fekrat**, None

* TJM and SF share senior authorship.

References

1. Armstrong MJ, Okun MS. Diagnosis and treatment of Parkinson disease: a review. *JAMA.* 2020;323(6):548–560.
2. Lebouvier T, Chaumette T, Paillusson S, et al. The second brain and Parkinson's disease. *Eur J Neurosci.* 2009;30(5):735–741.
3. Archibald NK, Clarke MP, Mosimann UP, Burn DJ. The retina in Parkinson's disease. *Brain.* 2009;132(5):1128–1145.
4. Armstrong RA. Oculo-visual dysfunction in Parkinson's disease. *J Parkinsons Dis.* 2015;5(4):715–726.
5. Mohana Devi S, Mahalaxmi I, Aswathy NP, Dhivya V, Balachandar V. Does retina play a role in Parkinson's disease? *Acta Neurol Belg.* 2020;120(2):257–265.
6. Biousse V, Skibell BC, Watts RL, Loupe DN, Drews-Botsch C, Newman NJ. Ophthalmologic features of Parkinson's disease. *Neurology.* 2004;62(2):177–180.
7. Altintaş O, Işeri P, Ozkan B, Cağlar Y. Correlation between retinal morphological and functional findings and clinical severity in Parkinson's disease. *Doc Ophthalmol.* 2008;116(2):137–146.
8. Ortuño-Lizarán I, Beach TG, Serrano GE, Walker DG, Adler CH, Cuenca N. Phosphorylated α-synuclein in the retina is a biomarker of Parkinson's disease pathology severity. *Mov Disord.* 2018;33(8):1315–1324.
9. Garcia-Martin E, Rodriguez-Mena D, Satue M, et al. Electrophysiology and optical coherence tomography to evaluate Parkinson disease severity. *Invest Ophthalmol Vis Sci.* 2014;55(2):696–705.
10. Beach TG, Adler CH, Lue L, et al. Unified staging system for Lewy body disorders: correlation with nigrostriatal degeneration, cognitive impairment and motor dysfunction. *Acta Neuropathol.* 2009;117(6):613–634.
11. Iadecola C. The neurovascular unit coming of age: a journey through neurovascular coupling in health and disease. *Neuron.* 2017;96(1):17–42.
12. Sweeney MD, Kisler K, Montagne A, Toga AW, Zlokovic BV. The role of brain vasculature in neurodegenerative disorders. *Nat Neurosci.* 2018;21(10):1318–1331.
13. Guan J, Pavlovic D, Dalkie N, et al. Vascular degeneration in Parkinson's disease. *Brain Pathol.* 2013;23(2):154–164.
14. Nanhoe-Mahabier W, de Laat KF, Visser JE, Zijlmans J, de Leeuw FE, Bloem BR. Parkinson disease and comorbid cerebrovascular disease. *Nat Rev Neurol.* 2009;5(10):533–541.
15. van der Holst HM, van Uden IW, Tuladhar AM, et al. Cerebral small vessel disease and incident parkinsonism: the RUN DMC study. *Neurology.* 2015;85(18):1569–1577.
16. Liew G, Wang JJ, Mitchell P, Wong TY. Retinal vascular imaging: a new tool in microvascular disease research. *Circ Cardiovasc Imaging.* 2008;1(2):156–161.
17. Kromer R, Buhmann C, Hidding U, et al. Evaluation of retinal vessel morphology in patients with Parkinson's disease using optical coherence tomography. *PLoS One.* 2016;11(8):e0161136.
18. Bittersohl D, Stemplewitz B, Keseru M, Buhmann C, Richard G, Hassenstein A. Detection of retinal changes in idiopathic Parkinson's disease using high-resolution optical coherence tomography and Heidelberg retina tomography. *Acta Ophthalmol.* 2015;93(7):e578–e584.
19. Shi C, Chen Y, Kwapong WR, et al. Characterization by fractal dimension analysis of the retinal capillary network in Parkinson disease. *Retina.* 2020;40(8):1483–1491.
20. Kwapong WR, Ye H, Peng C, et al. Retinal microvascular impairment in the early stages of Parkinson's disease. *Invest Ophthalmol Vis Sci.* 2018;59(10):4115–4122.
21. Miri S, Shrier EM, Glazman S, et al. The avascular zone and neuronal remodeling of the fovea in Parkinson disease. *Ann Clin Transl Neurol.* 2015;2(2):196–201.
22. Berkowitz S, Patel S. Pilot study for neurological and retinal imaging as biomarkers for Parkinson's disease using optical coherence tomography-angiography. *Invest Ophthalmol Vis Sci.* 2020;61(7):4831.
23. Ahn S, Shin J, Song SJ, et al. Neurologic dysfunction assessment in Parkinson disease based on fundus photographs using deep learning. *JAMA Ophthalmol.* 2023;141(3):234–240.
24. Kashani AH, Asanad S, Chan JW, et al. Past, present and future role of retinal imaging in neurodegenerative disease. *Prog Retin Eye Res.* 2021;83:100938.
25. Aydin TS, Umit D, Nur OM, et al. Optical coherence tomography findings in Parkinson's disease. *Kaohsiung J Med Sci.* 2018;34(3):166–171.
26. Elkhatib THM, Hashim NA, Emad EM, Zein H, El-aidy L. Optical coherence tomography and cognitive dysfunction in Parkinson disease. *Egypt J Neurol Psychiatr Neurosurg.* 2019;55(1):52.
27. Sengupta P, Dutta K, Ghosh S, Mukherjee A, Pal S, Basu D. Optical coherence tomography findings

in patients of Parkinson's disease: an Indian perspective. *Ann Indian Acad Neurol.* 2018;21(2):150–155.
28. Iafe NA, Phasukkijwatana N, Chen X, Sarraf D. Retinal capillary density and foveal avascular zone area are age-dependent: quantitative analysis using optical coherence tomography angiography. *Invest Ophthalmol Vis Sci.* 2016;57(13):5780–5787.
29. Laatikainen L, Larinkari J. Capillary-free area of the fovea with advancing age. *Invest Ophthalmol Vis Sci.* 1977;16(12):1154–1157.
30. Zou J, Liu K, Li F, Xu Y, Shen L, Xu H. Combination of optical coherence tomography (OCT) and OCT angiography increases diagnostic efficacy of Parkinson's disease. *Quant Imaging Med Surg.* 2020;10(10):1930–1939.
31. Robbins CB, Thompson AC, Bhullar PK, et al. Characterization of retinal microvascular and choroidal structural changes in Parkinson disease. *JAMA Ophthalmol.* 2021;139(2):182–188.
32. Soliman AZ, Silva PS, Aiello LP, Sun JK. Ultrawide field retinal imaging in detection, classification, and management of diabetic retinopathy. *Semin Ophthalmol.* 2012;27(5-6):221–227.
33. Postuma RB, Berg D, Stern M, et al. MDS clinical diagnostic criteria for Parkinson's disease. *Mov Disord.* 2015;30(12):1591–1601.
34. Postuma RB, Poewe W, Litvan I, et al. Validation of the MDS clinical diagnostic criteria for Parkinson's disease. *Mov Disord.* 2018;33(10):1601–1608.
35. Sagong M, van Hemert J, Olmos de Koo LC, Barnett C, Sadda SR. Assessment of accuracy and precision of quantification of ultra-widefield images. *Ophthalmology.* 2015;122(4):864–866.
36. Pellegrini E, Robertson G, MacGillivray T, van Hemert J, Houston J, Trucco E. A graph cut approach to artery/vein classification in ultra-widefield scanning laser ophthalmoscopy. *IEEE Trans Med Imaging.* 2018;37(2):516–526.
37. Pellegrini E, Robertson G, Trucco E, et al. Blood vessel segmentation and width estimation in ultra-wide field scanning laser ophthalmoscopy. *Biomed Opt Express.* 2014;5(12):4329–4337.
38. Annunziata R, Kheirkhah A, Aggarwal S, Cavalcanti B, Hamrah P, Trucco E. Tortuosity classification of corneal nerves images using a multiple-scale-multiple-window approach. In: *Ophthalmic Medical Image Analysis International Workshop Conference Proceedings*. 2014:113–120.
39. Pead E, Thompson AC, Grewal DS, et al. Retinal vascular changes in Alzheimer's dementia and mild cognitive impairment: a pilot study using ultra-widefield imaging. *Transl Vis Sci Technol.* 2023;12(1):13.
40. Huang F, Dashtbozorg B, Zhang J, et al. Reliability of using retinal vascular fractal dimension as a biomarker in the diabetic retinopathy detection. *J Ophthalmol.* 2016;2016:6259047.
41. Pead E, Giarratano Y, Tatham AJ, et al. 2D alpha-shapes to quantify retinal microvasculature morphology and their application to proliferative diabetic retinopathy characterisation in fundus photographs. *Sci Rep.* 2021;11(1):22814.
42. Frost S, Kanagasingam Y, Sohrabi H, et al. Retinal vascular biomarkers for early detection and monitoring of Alzheimer's disease. *Transl Psychiatry.* 2013;3(2):e233.
43. Stosić T, Stosić BD. Multifractal analysis of human retinal vessels. *IEEE Trans Med Imaging.* 2006;25(8):1101–1107.
44. Gulmez Sevim D, Unlu M, Sonmez S, Gultekin M, Karaca C, Ozturk Oner A. Retinal vessel diameter obtained by optical coherence tomography is spared in Parkinson's disease. *Int Ophthalmol.* 2019;39(4):813–819.
45. Han H-C. Twisted blood vessels: symptoms, etiology and biomechanical mechanisms. *J Vasc Res.* 2012;49(3):185–197.
46. Muraoka Y, Tsujikawa A, Kumagai K, et al. Retinal vessel tortuosity associated with central retinal vein occlusion: an optical coherence tomography study. *Invest Ophthalmol Vis Sci.* 2014;55(1):134–141.
47. Xie X, Wang Y, Zhu H, Zhou H, Zhou J. Impact of coronary tortuosity on coronary blood supply: a patient-specific study. *PLoS One.* 2013;8(5):e64564.
48. Black S, Gao F, Bilbao J. Understanding white matter disease: imaging-pathological correlations in vascular cognitive impairment. *Stroke.* 2009;40(3 suppl):S48–S52.
49. Thore CR, Anstrom JA, Moody DM, Challa VR, Marion MC, Brown WR. Morphometric analysis of arteriolar tortuosity in human cerebral white matter of preterm, young, and aged subjects. *J Neuropathol Exp Neurol.* 2007;66(5):337–345.
50. Ramos L, Novo J, Rouco J, Romeo S, Álvarez MD, Ortega M. Retinal vascular tortuosity assessment: inter-intra expert analysis and correlation with computational measurements. *BMC Med Res Methodol.* 2018;18(1):144.
51. Cheung CY-l, Ong YT, Ikram MK, et al. Microvascular network alterations in the retina of patients with Alzheimer's disease. *Alzheimers Dement.* 2014;10(2):135–142.
52. Einarsdottir AB, Hardarson SH, Kristjansdottir JV, Bragason DT, Snaedal J, Stefánsson E.

Retinal oximetry imaging in Alzheimer's disease. *J Alzheimers Dis.* 2016;49:79–83.
53. Nimmo J, Johnston DA, Dodart JC, et al. Perivascular pathways for clearance of α-synuclein and tau from the brain: implications for the pathogenesis of dementias and for immunotherapy. *Alzheimers Dement (Amst).* 2020;12(1):e12070.
54. Tamo W, Imaizumi T, Tanji K, et al. Expression of alpha-synuclein, the precursor of non-amyloid beta component of Alzheimer's disease amyloid, in human cerebral blood vessels. *Neurosci Lett.* 2002;326(1):5–8.
55. Murray CD. The physiological principle of minimum work: I. the vascular system and the cost of blood volume. *Proc Natl Acad Sci USA.* 1926;12(3):207–214.
56. Chawla A, Chawla R, Jaggi S. Microvasular and macrovascular complications in diabetes mellitus: distinct or continuum? *Indian J Endocrinol Metab.* 2016;20(4):546–551.
57. Faghihi H, Hajizadeh F, Riazi-Esfahani M. Optical coherence tomographic findings in highly myopic eyes. *J Ophthalmic Vis Res.* 2010;5(2):110–121.